Korean J. Chem. Eng., 36(5), 789-799 (2019)
DOI: 10.1007/s11814-019-0263-5

pISSN: 0256-1115
eISSN: 1975-7220

Networked column compartment model for a tilted packed column with structured packing

Yongho Son*,‡, Junhyung Park*,‡, Jisook Lee*, Kyungtae Park, and Wangyun Won***,†**

*Department of Chemical & Biomolecular Engineering, Sogang University, 35 Baekbeom-ro, Mapo-gu, Seoul 04107, Korea
**Department of Chemical and Biological Engineering, Sookmyung Women's University, 47 Cheongpa-ro, Yongsan-gu, Seoul 04310, Korea
***Department of Chemical Engineering, Changwon National University, 20 Changwondaehak-ro, Uichang-gu, Changwon, Gyeongnam 51140, Korea
(*Received 19 January 2019 • accepted 1 April 2019*)

Abstract−To successfully implement floating liquefied natural gas technology (FLNG), the separation columns on the topside of FLNG must be optimally designed. To this end, a reliable model that can predict column performance in offshore environments is needed. In this study, a networked column compartment model (NCCM), based on 2D-liquid and gas distribution models (LGDM), was proposed as a reliable offshore column model. A pilot-scale experiment for a column with structured packing was conducted to obtain experimental data regarding the absorption performance of the column in offshore environments. The results of the NCCM were compared with the experimental data. With the aid of the developed model, the effect of tilt angles on absorption performance and packed height was quantified.

Keywords: Offshore Column, CO_2 Absorption, Natural Gas, Sloshing Machine, FLNG

INTRODUCTION

The global demand for liquefied natural gas (LNG) has increased as it is cleaner than other fossil fuels [1-3]. Floating liquefied natural gas (FLNG) technology, which is an economically feasible method of exploiting stranded offshore gas wells, has also received increasing attention [4,5]. Yet, further research should be conducted on FLNG, particularly regarding the design of their topsides that suffer from exposure to offshore environments [6]. Although separation columns installed on the topsides of FLNG have been operated for several decades under onshore conditions [7,8], the effects of offshore environments on the separation processes are not well-studied. For efficient column design, it is imperative that a reliable model that can predict the performance of these columns in offshore environments is developed.

A reliable offshore column model should be composed of the two separate models, a liquid and gas distribution model (LGDM) and a column performance model based on it. This is because the effect of the same maldistributions on column performance differs between chemical systems [9]. The LGDM should predictively provide the actual extent of maldistribution in a packed column, and the column performance model must consider the sensitivity of maldistribution on the performance of the column. In addition, the development of each model should be based on the experimental data obtained from the same experimental configuration [10]. In this study, we focused on the development of the column performance model.

A few studies have examined column performance models considering liquid maldistribution. They can be classified into parallel column [11-14], bypass [15,16], and first principle approach models [17,18]. The parallel column model uses two or more columns with different liquid flow rates determined from the extent of maldistribution. The parallel column model can show the effect of maldistribution on column performance, but the results are strongly dependent on the parameters used in the model. The bypass model assumes that a certain amount of liquid or gas pass a separation column without any mass transfer. The limitation of the bypass model is that it is difficult to estimate the actual amount of bypassed liquid or gas. The first principle approach model uses computational fluid dynamics (CFD) to determine maldistribution and its effects on the column performance, but there have been no supporting experimental data for the developed models.

In this study, we propose a column performance model composed of many networked sub-columns in a 2D-domain, based on the predictive LGDM, under permanent tilt. For the LGDM, we used the liquid and gas distribution models based on volume cells, representing the genuine geometry of a column with structured packing in 2D-space [19]. To tune the key parameters of the proposed model, we conducted a pilot-scale experiment using a packed column with a 0.4-m inner diameter and 4-m packed height on a sloshing machine that can simulate offshore conditions. The results of the NCCM were compared to the experimental data, and we found that both sets of data agreed well. In addition, quantitative analyses, such as the effect of tilt angle on the absorption efficiency and packed height, were conducted with the aid of the proposed model.

†To whom correspondence should be addressed.
E-mail: wwon@changwon.ac.kr
‡Equally contributed.

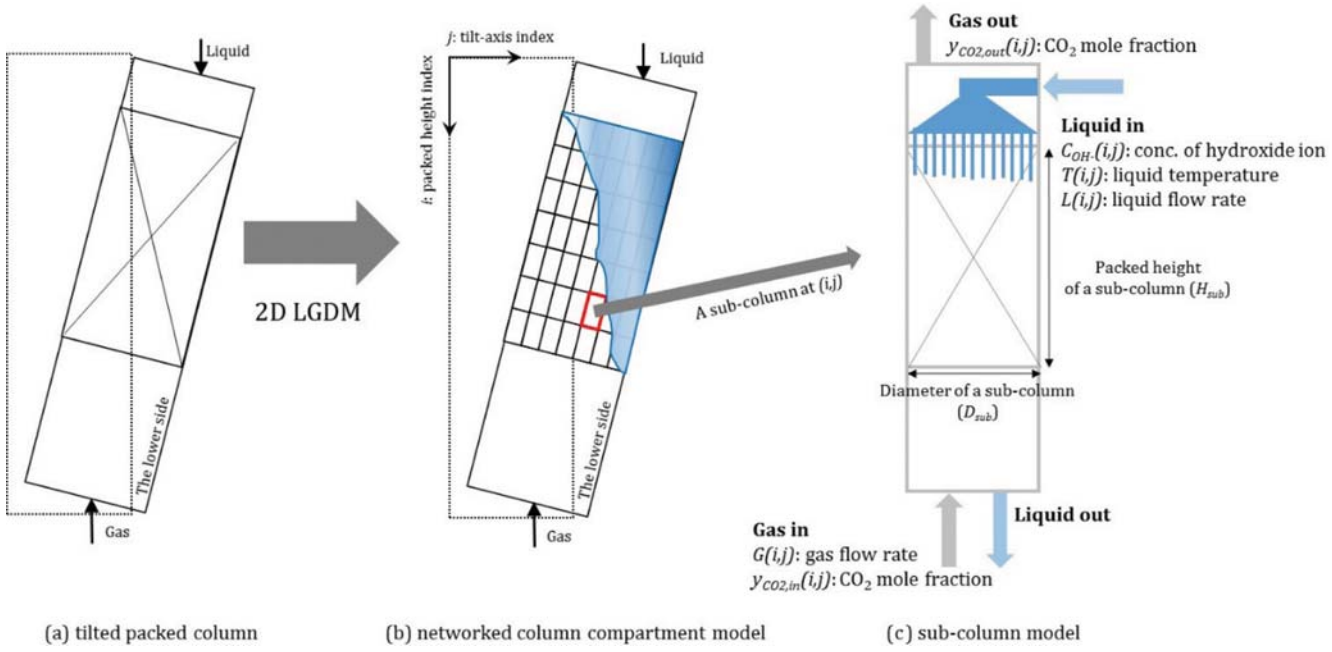

Fig. 1. Model framework of the networked column compartment model. (a) Tilted packed column, (b) networked column compartment model, and (c) sub-column model.

NETWORKED COLUMN COMPARTMENT MODEL (NCCM)

1. Model Overview

We propose a networked column compartment model (NCCM) for a tilted, packed column. The overview of the NCCM is shown in Fig. 1. A single tilted packed column is represented as smaller, 2D networked sub-columns through the LGDM. The corresponding liquid and gas distributions in the 2D sub-columns are calculated using the LGDM proposed for an offshore column [19]. The governing and constitutive equations for the relevant absorption system are applied to the sub-columns. In addition, the networking algorithm for liquid and gas streams in the sub-columns is developed and incorporated in the NCCM. The underlying premise of the NCCM is that the sub-column delimited by red lines in Fig. 1(b) can be approximated to a vertical packed column, as represented in Fig. 1(c). Under this premise, the dimension of a sub-column approximated to a vertical column, referred to as the vertical subcolumn dimension (VSD), is determined. In the proposed model, the VSD is introduced as a key parameter of NCCM to be tuned using experimental data. The following subsections will elucidate the main components comprising the NCCM.

2. Liquid and Gas Distribution Model (LGDM)

An LGDM for a tilted packed column was developed based in the 3D volume cell domain [19]. Using given column dimensions (such as the diameter and packed height), packing type, and operating conditions (such as liquid and gas flow rates), the LGDM can calculate the distribution of liquid and gas in the 3D volume cell domain. In the LGDM, the original dimension of a volume cell is determined by the geometry of the packing type, which is typically at the millimeter scale. Based on the unit dimension of a volume cell, a larger dimension can be obtained by grouping and summing the adjacent volume cells. Under the given VSD, the liquid and gas flow rates in the sub-columns are calculated using the LGDM with the grouping and summing.

3. Governing and Constitutive Equations

Governing and constitutive equations were established and applied to all generated sub-columns in the NCCM. The chemical system considered in this study absorbs CO_2 from atmospheric air into an aqueous NaOH solution. The chemical reactions of this system are as follows:

$$CO_2(aq)+2OH^- \rightarrow CO_3^{2-}+H_2O \quad (1)$$

$$r=k_{OH^-}[OH^-][CO_2]=k_1[CO_2] \quad (2)$$

At an excessive hydroxide concentration, the bicarbonate (HCO_3^-) is negligible. The rate expression of the reaction treated as pseudo-first-order can then be represented as Eq. (2).

The major assumptions of the model include the following:

(i) The hydroxide concentration within a subcolumn is constant.

(ii) Liquid flow rate (L), gas flow rate (G) and overall mass transfer coefficient (K_G) are constant within a sub-column.

(iii) Isothermal conditions are assumed within a sub-column.

(iv) The partial pressure of the CO_2 equilibrium in the liquid phase is zero.

The dilute CO_2 system allows the use of the first, third, and fourth assumptions. In addition, the underlying premise of the approximation of a subcolumn to a vertical column is the basis of the second assumption. Based on the above assumptions, the differential CO_2 mass balance associated with absorption in a subcolumn is written as:

$$u_G\frac{dy}{dz}=(K_Ga_e)(RT)(y^*-y) \quad (3)$$

Table 1. Constitutive equations for the overall mass transfer coefficient in Eq. (7)

Relevant value	Correlation used
Reaction rate constant (k_{OH^-})	$\log\left(\frac{k_{OH^-}}{k^{\infty}_{OH^-}}\right)=0.221I-0.016I^2$ [27]
	$\log k^{\infty}_{OH^-}=11.895-\frac{2382}{T}$
Diffusion coefficient ($D_{CO_2,L}$)	$D_{CO_2,L}=\frac{D_{CO_2,w}\mu_w}{\mu_L}$ [27]
	$\log_{10}D_{CO_2,w}=-8.1764+\frac{712.5}{T}-\frac{2.591\times10^5}{T^2}$
	$\mu_w=0.02414\cdot10^{\left(\frac{247.8}{T-140}\right)}$
	$\log_{10}\mu_L=\frac{878.159}{T}-3.0254+0.1103([OH^-]+2[CO_3^{2-}])+0.08947\left(\frac{[CO_3^{2-}]}{0.5[OH^-]+[CO_3^{2-}]}\right)$ [28]
Henry's constant (H_{CO_2})	$H_{CO_2}=\frac{1}{H_{CO_2-PM}}$; $\log\left(\frac{H_{CO_2-PM}}{H_{CO_2,w-PM}}\right)=-\sum I_i h_i$
	$I=\frac{1}{2}\sum c_i z_i^2$
	$h=h_+ + h_- + h_G$
	$\log H_{CO_2,w-PM}=9.1229-5.9044\cdot10^{-2}T+7.8857\cdot10^{-5}T^2$ [27]
	$\sum I_i h_i=I_{NaOH}(h_{Na^+}+h_{OH^-}+h_{CO_2})+I_{Na_2CO_3}(h_{Na^+}+h_{CO_3^{2-}}+h_{CO_2})$ [23]
	Contributions of other species (h_{Na^+}, h_{OH^-}, and $h_{CO_3^{2-}}$) can be found in [29]
	$h_{CO_2}=(4.364\cdot10^{-7})[T(^oC)]^3-(3.297\cdot10^{-5})[T(^oC)]^2+(1.204\cdot10^{-4})[T(^oC)]-6.847\cdot10^{-3}$

Using assumption (iv), Eq. (3) can be written as:

$$u_G\frac{dy}{dz}=(K_G a_e)(RT)(-y) \tag{4}$$

Integrating both sides of Eq. (4) and rearranging them to include $y_{CO_2,out}$ generates:

$$y_{CO_2,out}=\exp\left(\ln(y_{CO_2,in})-\frac{K_G a_e H_{sub} RT}{u_G}\right) \tag{5}$$

The effective surface area (a_e) correlation is determined following Billet and Schulte [20]:

$$a_e=1.5(a d_h)^{-0.5}\left(\frac{u_L d_h}{v_L}\right)^{-0.2}\left(\frac{u_L^2\rho_L d_h}{\sigma_L}\right)^{0.75}\left(\frac{u_L^2}{g d_h}\right)^{-0.45} \tag{6}$$

For pseudo-first-order reactions, the overall mass transfer coefficient (K_G) can be expressed via the negligible gas resistance [21], surface renewal theory [22,23] enhancement factor (E), and the Hatta number (Ha) as follows [24,25]:

$$K_G=k_g'=\frac{\sqrt{k_{OH^-}[OH^-]D_{CO_2,L}}}{H_{CO_2}} \tag{7}$$

The validity of Eq. (7) was tested experimentally by Tsai et al. [26] in a wetted-wall column experiment. They reported that the experimental results were less than ±9% of the predicted value using Eq. (7). The equations constituting the reaction rate constant (k_{OH^-}), diffusion coefficient of CO_2 in the liquid phase ($D_{CO_2,L}$), and Henry's constant (H_{CO_2}) are tabulated in Table 1.

In summary, Eq. (5) is implemented in a subcolumn with Eqs. (6) and (7), and the constitutive equations in Table 1, to calculate the CO_2 concentration at the gas outlet ($y_{CO_2,out}$) of a sub-column.

4. Stream Networking Algorithm

Owing to the 2D networked structure, the calculated CO_2 and hydroxide concentrations in the gas and liquid streams leaving the subcolumns are split and mixed with those of the other associated streams as liquid and gas flow through a tiled packed column. To account for this effect, a stream networking algorithm is developed. To simplify the stream networking algorithm, two assumptions are made:

(i) The hydroxide concentration changes only between the subcolumns.

(ii) Mixing and splitting of streams is only possible between laterally adjacent sub-columns.

The two assumptions are shown in Fig. 2. For the first assumption, hydroxide consumption is considered to occur between the sub-columns, as indicated by the black point in Fig. 2(a). The second assumption is that almost all portions of the split streams flow to the adjacent sub-columns, which are connected by the possible routes indicated by the colored arrows in Fig. 2(b).

From the above two assumptions and the given 2D liquid and gas distributions with the determined VSD, the gas split ratios (α) under tilted condition are simplified as shown in Fig. 3. When the column is tilted towards the left, as shown in Fig. 3, gas flowing

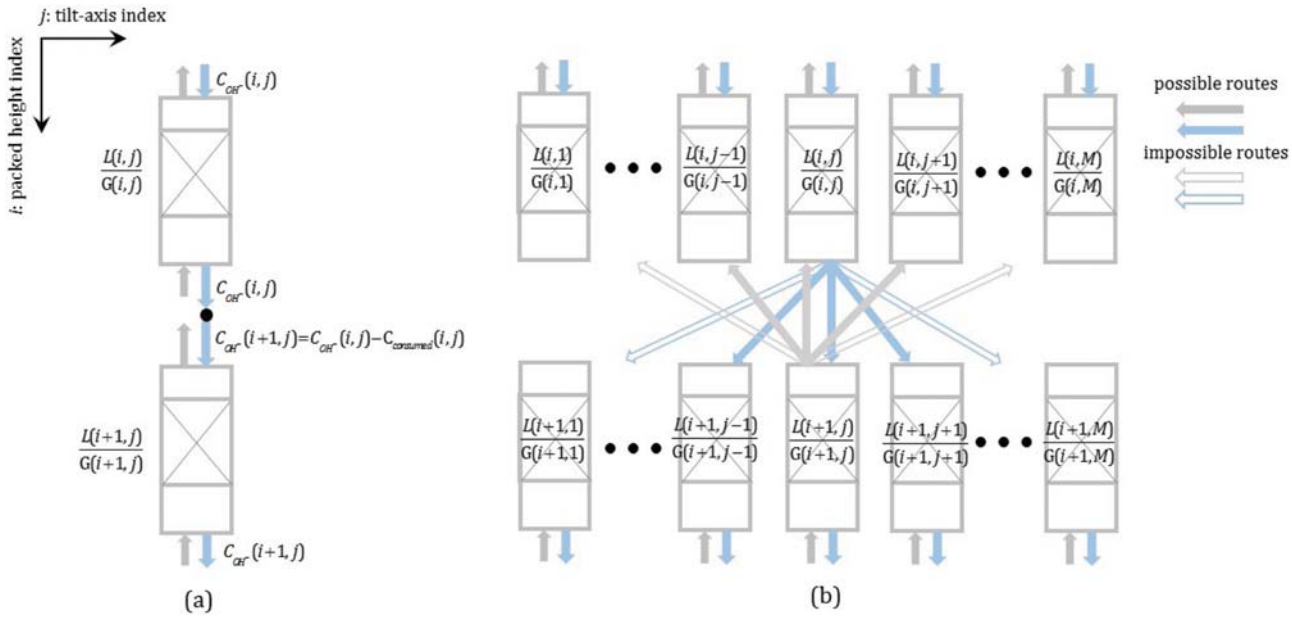

Fig. 2. Two assumptions for the stream networking algorithm. (a) Change in hydroxide concentration and (b) adjacent networking.

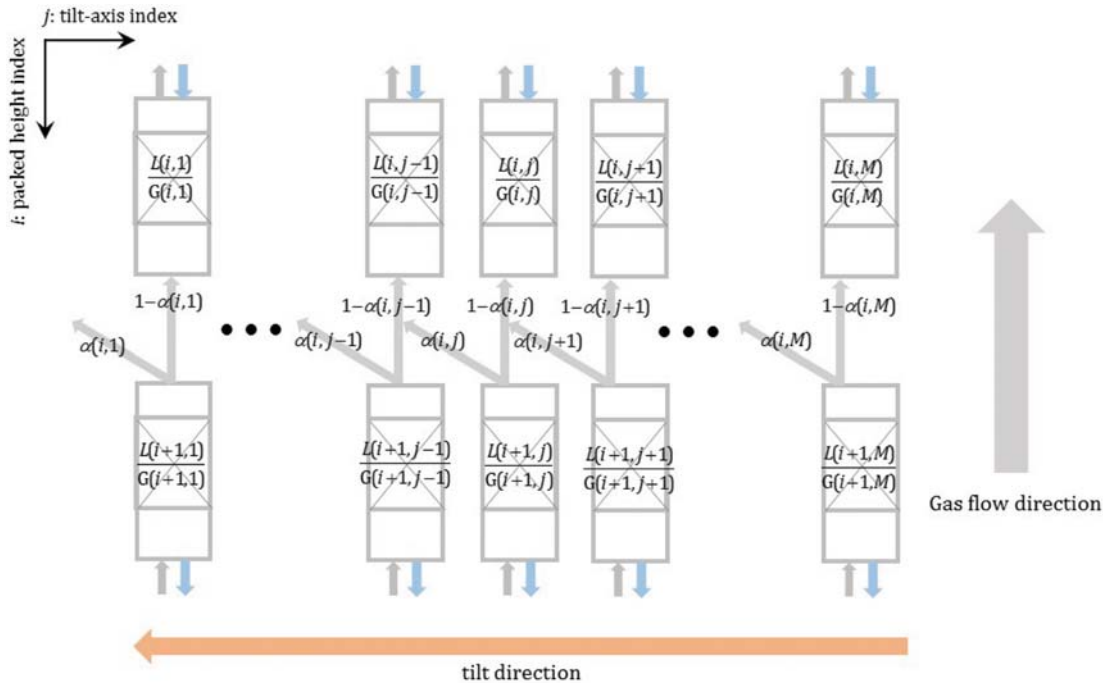

Fig. 3. Split ratios of gas streams in the steam networking algorithm.

upwards steadily moves towards the tilt direction along the packed height. It is because liquid holdup at the tilt direction is decreased from the bottom to the top and the more gas favorably flows the lower resistance region as flowing upwards. On the other hand, liquid flowing downwards moves towards the tilt direction. The labeled ratios of the gas stream can be expressed using the calculated gas flow rates of the sub-columns as follows:

$$A_G(i)x_G(i)=b_G(i) \text{ for i=1 (top) to N (bottom)} \quad (8)$$

where

$$A_G(i)=\begin{bmatrix} G(i+1,1) & 0 & 0 & 0 & 0 \\ & \ddots & & & \\ 0 & G(i+1,j-1) & -G(i+1,j) & 0 & 0 \\ 0 & 0 & G(i+1,j) & -G(i+1,j+1) & 0 \\ 0 & 0 & 0 & G(i+1,j+1) & 0 \\ & & & & \ddots \\ 0 & 0 & 0 & 0 & G(i+1,M) \end{bmatrix}$$

$$x_G(i)=\begin{bmatrix}\alpha(i,1)\\ \vdots\\ \alpha(i,j-1)\\ \alpha(i,j)\\ \alpha(i,j+1)\\ \vdots\\ \alpha(i,M)\end{bmatrix},\ b_G(i)=\begin{bmatrix}G(i+1,1)-G(i,1)\\ \vdots\\ G(i+1,j-1)-G(i,j-1)\\ G(i+1,j)-G(i,j)\\ G(i+1,j+1)-G(i,j+1)\\ \vdots\\ G(i+1,M)-G(i,M)\end{bmatrix}$$

where N is the column bottom index of packed height index. The equation for the liquid stream split ratios can be formulated in the same way. The gas ratio vector (x_G) can be calculated by multiplying the inverse matrix of gas flow rates (A_G) of both sides.

5. Parameter Estimation

Two parameters are introduced to the NCCM. The first is the VSD, including the diameter (D_{sub}) and packed height (H_{sub}) of a vertical sub-column. The second is the adjustable factor for the correlation of the effective surface area. Although the Billet and Schulte [20] area correlation is commonly used and reliable for a column with structured packing, it is more appropriate to assume that there would be a suitably tailored area correlation for our experimental data. This is because the area correlation is applied to all generated subcolumns, which have significantly smaller dimensions to the experimental columns used when the Billet and Schulte [20] correlation was derived. The area correlation is corrected by the liquid load correction function in a sub-model as a form of $\lambda_1 L(i,j)^{\lambda_2}$. Thus, the decision variable vectors are composed of the four parameters. $X=[D_{sub}, H_{sub}, \lambda_1, \lambda_2]$. The objective function is formulated using the sum of the squared error of the CO_2 concentration at the column outlet between the model and the experimental data as follows:

$$\min_{\Theta} J=\sum_{k=1}^{K_{exp}}\left(y_k-y_k^{NCCM}(X)\right)^2 \quad \text{subject to } X_{min}\le X\le X_{max} \quad \text{Eqs. (5) to (7)} \tag{9}$$

where y_i and y_i^{NCCM} indicate the experimental measurements and

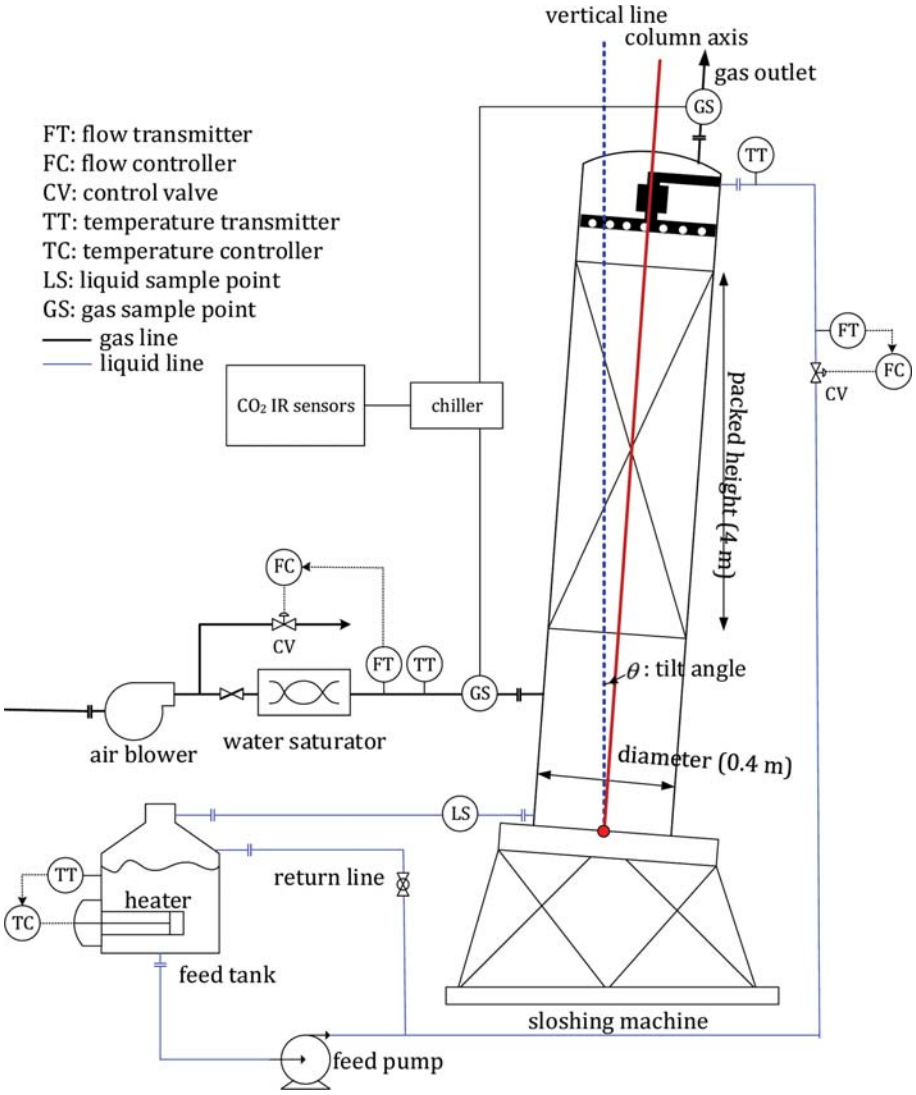

Fig. 4. Experimental packed column.

the NCCM's results of the outlet CO_2 concentration during the k^{th} experimental run, respectively, and X denotes the decision variable vector to be estimated. K_{exp} is the number of experimental runs. To solve the above constrained optimization, a sequential quadratic programming (SQP) method was used [30,31].

EXPERIMENTS

1. Experimental Packed Column

Fig. 4 shows the experimental packed column with the instruments and other equipment. The packed column, with a 0.4-m diameter and 4-m packed height, is installed on a sloshing machine which can implement offshore conditions. Twelve stainless steel (SS) and eight polypropylene (PP) TSP250X, similar to Mellapak 250X, are used for the structured packing, which is the same configuration where the LGDM was developed [32]. The drip density of liquid distributor is 167 drips/m^2, which is enough to create an even liquid distribution [33]. In addition to the equipment configuration for the liquid and gas distribution experiment, IR CO_2 sensors are installed at both the inlet and outlet gas lines to measure the CO_2 concentration. A liquid is sampled from the liquid outlet and analyzed using a pH meter to measure the concentration of hydroxide ions at each experimental run.

Aqueous 0.1-M NaOH was prepared by dissolving solid NaOH pellets in the feed tank. The solution was mixed through the return line connecting the liquid feed pump and tank. It took approximately 12 hours to create a homogeneous 0.1-M NaOH solution for 4 m^3 of liquid. After the mixing step, the solution was checked by neutralization titration with 1-M HCl to determine if the mixed solution had the desired concentration (0.1 M) in both the feed tank and liquid outlet. The temperature of the prepared solution was maintained at 28 °C in the feed tank using a temperature control loop. After preparing the NaOH solution in the feed tank, prewetting was conducted with a higher liquid load (approximately 55 m^3/m^2 hr), which is a common practice during industrial packed column operation [21]. Whenever the hydroxide concentration dropped below 0.06 M, we discarded the remaining solution and prepared a fresh 0.1 M NaOH solution to prevent interfacial reactant depletion in the experimental column that could occur at lower hydroxide concentrations.

Table 2. Main experimental conditions

Condition	Value
Mean liquid load (m^3/m^2/hr)	14, 32, 50
Gas factor ($Pa^{0.5}$)	1, 2, 3
Permanent tilt (θ, degrees)	0, 2, 4, 6
Initial concentration of aqueous NaOH (mol/L)	0.1

*Column operating temperature and pressure: 28 °C and 1 bara

The desired liquid load was first set and flowed through the column before gas at the desired flow rate. The gas then flowed through the column at the desired flow rate. When the main real-time measurements, such as the liquid and gas flow rates, and CO_2 concentrations, at both the inlet and outlet were constant, the experimental run was complete and the liquid was collected at the outlet of the column for sampling. The liquid load was changed incrementally to prevent the effect of a static holdup from the previous run. The static holdup may have influenced absorption performance if the liquid load had changed in a decremental manner [21]. Whenever the liquid load should be changed in a decremental manner, column saturation is conducted by flowing a gas without liquid until the CO_2 concentration is the same at the inlet and outlet to eliminate the effect of the static holdup. The main experimental conditions are tabulated in Table 2.

RESULTS AND DISCUSSION

1. Vertical NCCM Results

Fig. 5(a) shows a parity plot of the NCCM results and experimental data under a vertical condition. The results calculated using the NCCM are within the ±5% deviation lines of the corresponding experimental data. The adjusted effective surface area is shown in Fig. 5(b) and compared with the other two area correlations that are commonly used for a column with structured packing. The estimated key VSD parameters under the vertical condition are 0.11 m and 0.02 m for the packed height and diameter, respectively. The estimated diameter of the sub-column was even smaller

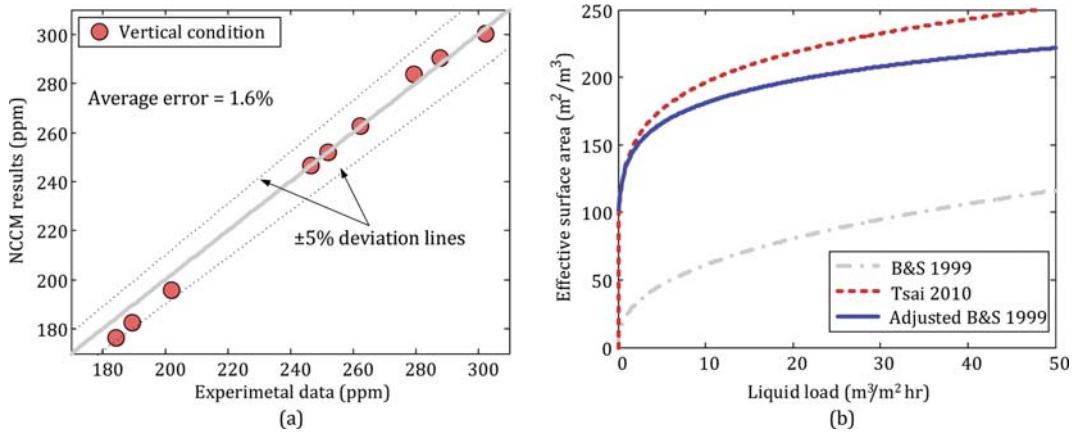

Fig. 5. Vertical column results (a) parity plot of the NCCM results and experimental data under a vertical condition, and (b) adjusted effective surface area and other area correlations.

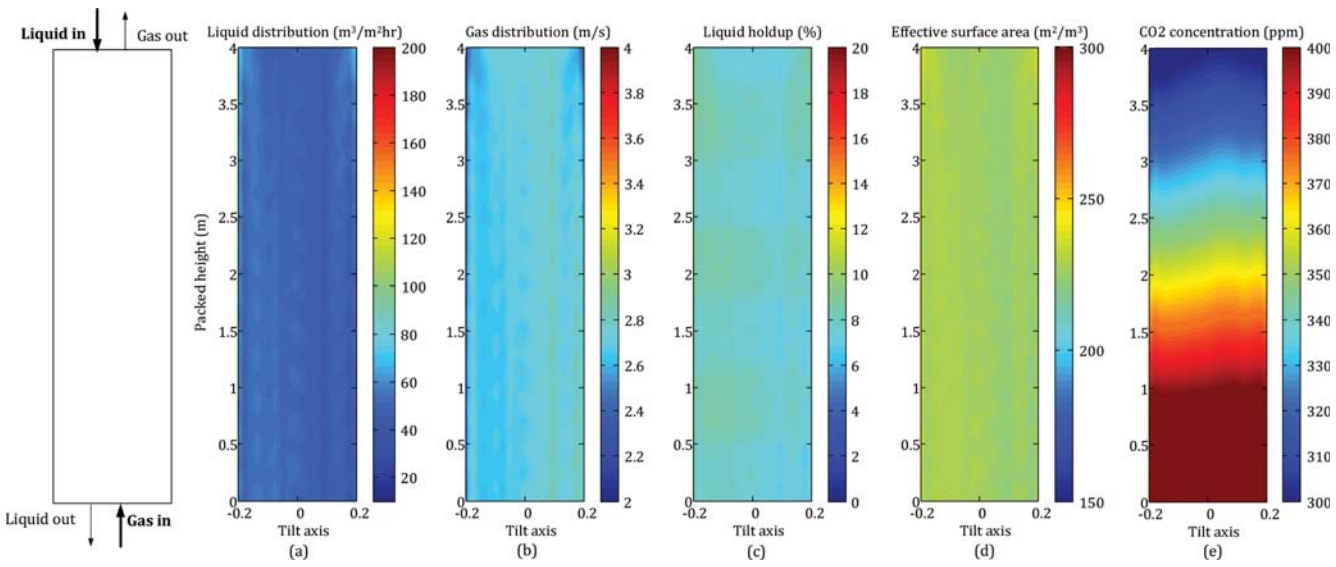

Fig. 6. Two-dimensional results of the NCCM with a 2D hydraulic model under a vertical condition at L=50 m^3/m^2 hr, G=3 $Pa^{0.5}$. (a) Liquid distribution (m^3/m^2 hr), (b) gas distribution (m/s), (c) liquid holdup (%). (d) effective surface area (m^2/m^3), and (e) CO_2 concentration (ppm).

than the packed height. This means that averaging along the tilt axis has a greater influence on absorption performance than that along the packed height axis. By adjusting the area correction function, the trend and magnitude of the base effective surface area model with a liquid load could be modified so that the results of the NCCM agreed well with the corresponding experimental data. The adjusted effective surface area is close to that reported by Tsai 2010, which was developed based solely on structured packing and more close to our experimental data. From these facts, we could conclude that the adjusted area correlation is reasonable. The slightly lower magnitude of the adjusted area correlation than that reported by Tsai 2010 could be due to the mixed materials with PP and SS in the experimental column.

Two-dimensional results were obtained from the NCCM with the 2D LGDM, which can calculate liquid, gas, and liquid holdup distributions, as shown in Fig. 6(a)-(c). For a vertical column, the calculated liquid and gas distributions are almost even throughout the packed bed. Based on the 2D LGDM results, the 2D distributions of the effective surface area and CO_2 concentration were calculated, as shown in Figs. 6(d) and 6(e), respectively. As the liquid is distributed evenly, the effective surface area is almost constant over the 2D domain. The CO_2 concentration of the feed gas that entered at H=0 steadily decreased as it flowed upwards without any noticeable non-uniformity caused by the tilt axis. In this vertical case, the outlet CO_2 concentration was calculated to 298 ppm. From these results, we could conclude that the absorption performance of a vertical column can be simulated using the one-dimensional mass and heat balance along the packed height without any consideration of the lateral axis, as already implemented in commercial simulation software, such as Aspen Plus and ProMax.

2. Tilt NCCM Results

Fig. 7 compares the absorption performance of a tilted packed column calculated by the NCCM are with the corresponding experimental data. Note that the NCCM results for a tilted packed column were obtained using the VSD and adjusted effective surface area obtained from the vertical NCCM without any additional correction. The effect of tilt on the absorption performance is represented by the 2D LGDM. The average error between the calculated NCCM results and experimental data is 1.5%. Almost all calculated results are located on the diagonal line. This demonstrates that the NCCM with the VSD and adjusted effective surface area can describe the experimental absorption performance of a tilted packed column well.

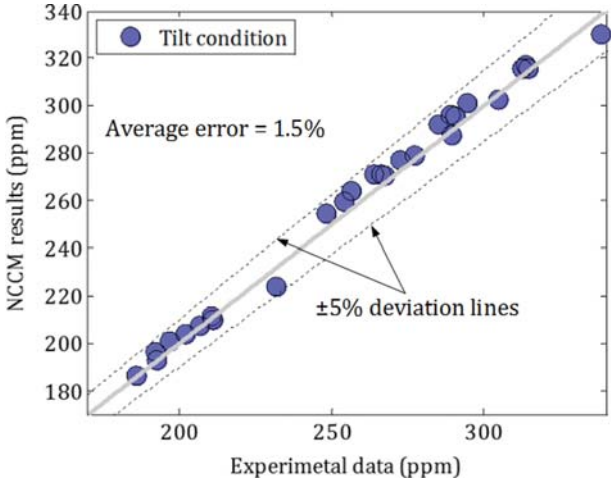

Fig. 7. Parity plot of the NCCM's results and experimental data under tilted conditions.

The two-dimensional results were obtained at a tilt angle of 6° using the NCCM and 2D LGDM, as shown in Fig. 8. Unlike the vertical result in Fig. 6(a), the liquid distribution is significantly skewed towards the tilt axis, as shown in Fig. 8(a). Correspondingly, gas and liquid holdup is severely maldistributed. The significant liquid maldistribution deteriorates the uniformity of the effective

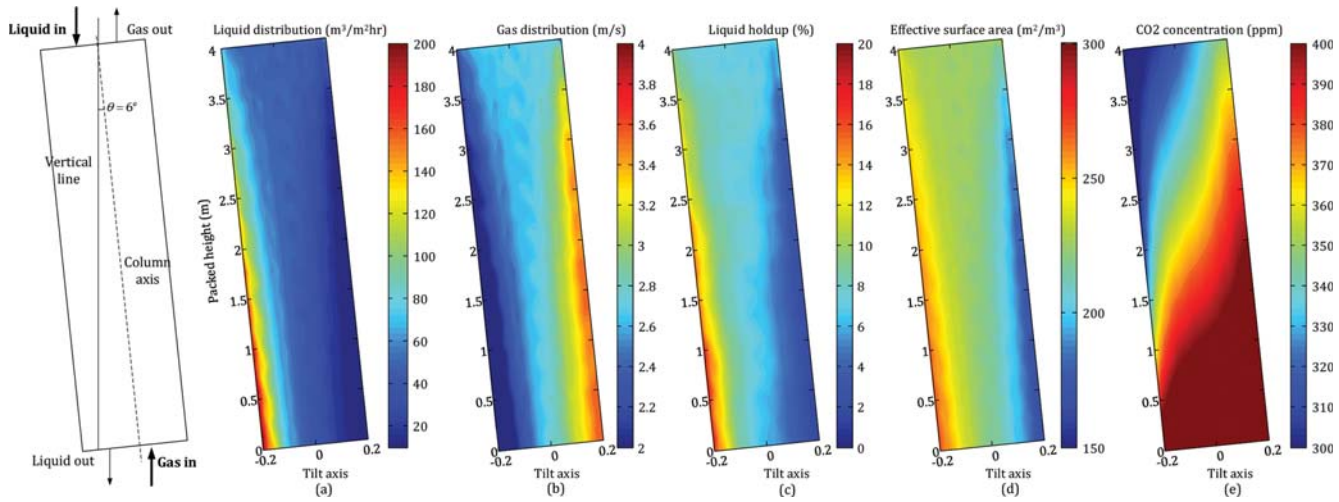

Fig. 8. Two-dimensional results of the NCCM with a 2D hydraulic model at tilt angle=6° and L=50 m^3/m^2 hr, G=3 $Pa^{0.5}$. (a) Liquid distribution (m^3/m^2 hr), (b) gas distribution (m/s), (c) liquid holdup (%), (d) effective surface area (m^2/m^3), and (e) CO_2 concentration (ppm).

surface area in the 2D domain, creating a higher effective surface area at the inclined lower wall region. Based on these results, the resulting CO_2 concentration in a packed column with a 6° tilt angle is shown in Fig. 8(e). At the inclined lower wall region, where the higher liquid load and lower gas flow rates are interacting, CO_2 is absorbed deeply. However, at the counterpart region, where gas channeling is profound, the CO_2 absorption performance is lower. The two opposing effects combined to create an overall lower absorption performance than that at vertical conditions; the tilted conditions resulted in a CO_2 concentration of 311 ppm, while the vertical conditions resulted in a concentration of 298 ppm. This indicates that the decrease in the CO_2 absorption at the upper wall region is more significant than the increased CO_2 absorption at the inclined lower wall region. These results show that the 1D modeling approach to obtain absorption performances is not feasible for a tilted packed column as they cannot consider the spatial asymmetry of the liquid, gas, and effective surface area as illustrated in Fig. 8.

3. Quantitative Analysis of the Effect of Tilt Angle on Absorption Performances

Using the adjusted NCCM, the effect of tilt on the absorption performance can be quantified more accurately. In this work, we propose two metrics for quantifying the effect of tilt effect on absorption performance. The first is the mass transfer efficiency, which is defined as the volumetric mass transfer coefficient at tilted conditions over that in a vertical column, as follows:

$$\text{Mass transfer efficiency } (\eta_{mte}) = (K_g a_e)_{tilt} / (K_g a_e)_{ver}.$$

While the volumetric mass transfer coefficient under tilted conditions is directly calculated from the experimental data, the vertical column parameters are calculated from the vertical NCCM. This approach can calculate a more accurate efficiency than that from experimental data for both conditions as it would be impossible to apply the same operating conditions to pilot-scale experiments, except tilt angle. The differences in operating conditions would render the actual effect of tilt angle on absorption performance unclear. Thus, the vertical results were calculated with the aid of the model by inputting the same operating conditions used in the corresponding tilt experiment run.

Fig. 9 shows the mass transfer efficiency in terms of permanent tilt angle for an NaOH-air absorption system at L=14, 32, 50 m^3/m^2 hr, tilt angle=0, 2, 4, 6°, and F_g=1, 2, 3 $Pa^{0.5}$. Under the considered operating conditions, the mass transfer efficiency decreased to approximately 0.85 as the tilt angle increased. In addition, the effect of tilt angle intensified as L/F_g increased. The reason for the detrimental effect of tilt angle at higher L/F_g could be explained from liquid and gas maldistribution. Son et al. reported that liquid maldistribution is detrimental as the liquid load is decreased and gas load is increased (i.e., higher L/F_g) in a tilted column with structured packing [32].

4. Quantitative Analysis of the Effects of Tilt Angle on Packed Height

Using the proposed NCCM, the effects of tilt angle on packed height were investigated. First, the required packed height to achieve the same absorption performance of the NaOH-air system under tilt conditions were calculated using the NCCM, as shown in Fig. 10(a). The operating conditions are L=50 m^3/m^2 hr, G=3 $Pa^{0.5}$. The required packed height of a tilted packed column to meet the same absorption performance of a vertical column was steadily extended as tilt angle increased. That is, at the same packed height, a tilted packed column cannot achieve the same absorption performance as a vertical column due to the detrimental effects of tilt angle. At a tilt angle of 6°, the packed height should be increased to 1.28 times that of the vertical column.

To quantify the effect of tilt on the required packed height, a different index for absorption performance, denoted as absorption efficiency, is introduced, which is defined as the packed height of a vertical column over the required packed height of a tilted column to achieve the same absorption performance.

$$\text{Absorption efficiency } (\eta_{ae}) = H_{ver} / H_{tilt}$$

The advantage of this metric is that it can be directly used to calculate the required packed height for a tilted packed column. How-

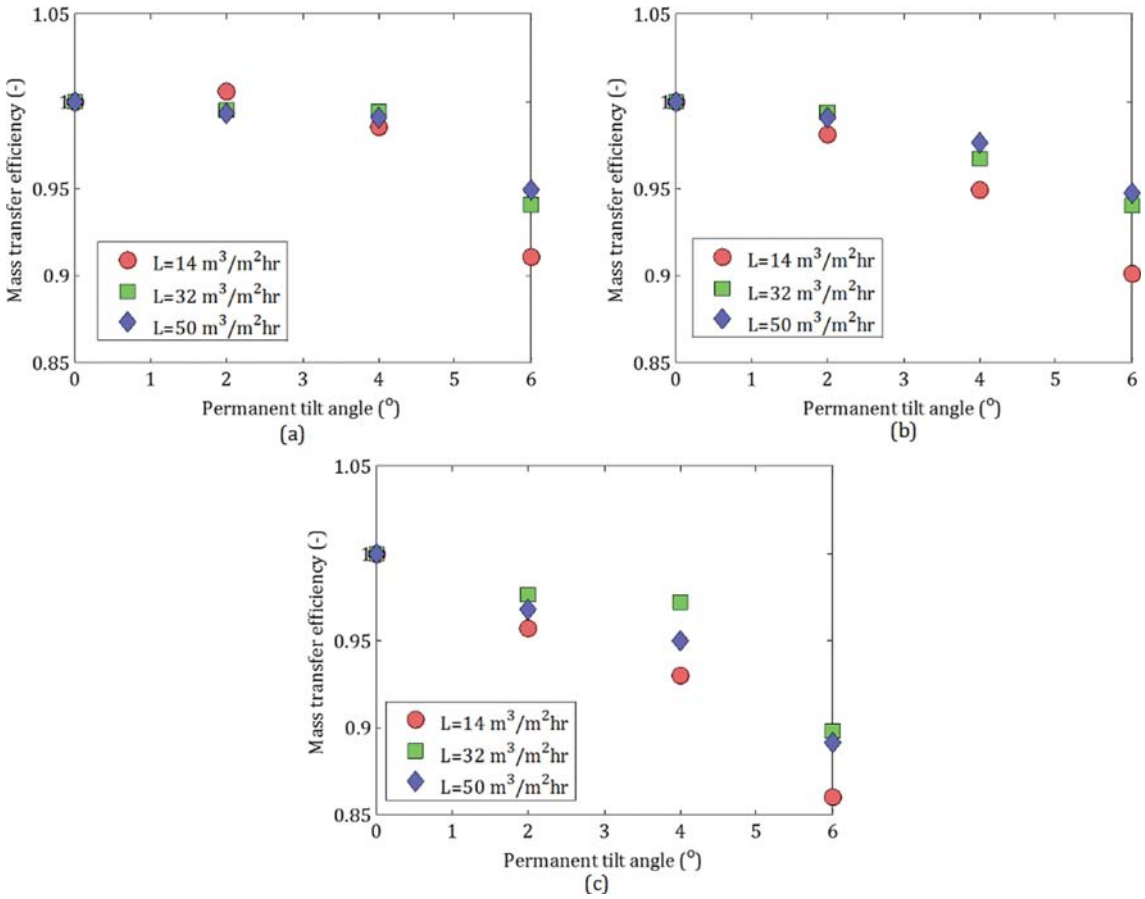

Fig. 9. Effects of tilt angle on absorption performances. (a) F_g=1, (b) F_g=2, and (c) F_g=3 $Pa^{0.5}$.

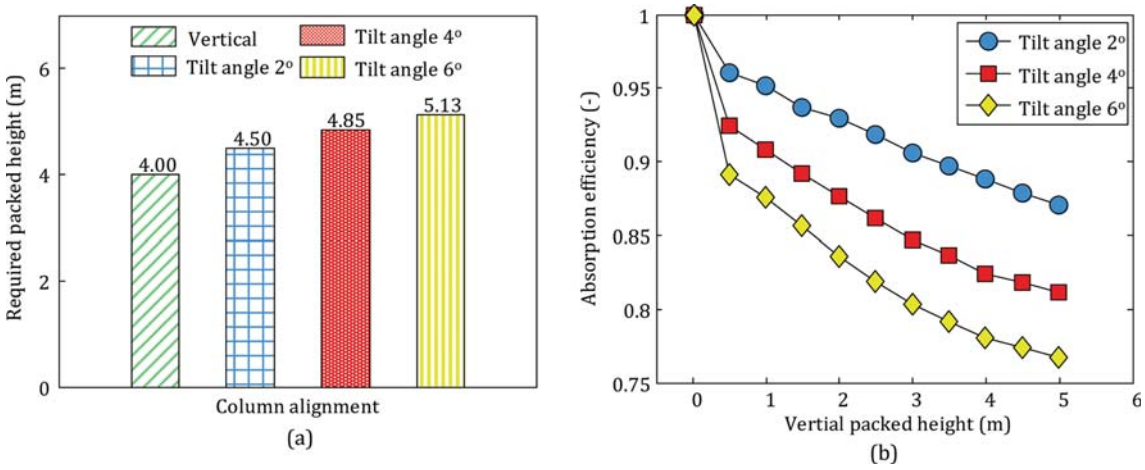

Fig. 10. Effects of tilt angle on packed height. (a) Required packed height under tilted conditions, and (b) absorption efficiency with an increment of a packed height.

ever, it can only be obtained with the aid of a reliable absorption model for a tilted packed column, such as the NCCM. As shown in Fig. 10(a), the calculated absorption efficiencies were 0.89, 0.82, and 0.78 for tilt angles of 2°, 4°, and 6°, respectively.

Fig. 10(b) shows that the absorption efficiency decreases under all considered tilt angles as the vertical packed height increases. This indicates that the effect of tilt on packed height is more detrimental at deeper packed heights. This is because liquid and gas mal-distribution worsened as packed height increased within the same column diameter. These results also suggest that the effect of tilt angle on the required packed height is a function of the dimensions of column: column diameter and packed height. The advantage of the NCCM with the two-dimensional LGDM is that it can incorporate fluid maldistribution as a function of column dimen-

sions. Thus, the proposed model can appropriately describe the worsened absorption performance at different packed heights.

CONCLUSIONS

We have proposed a two-dimensional column performance model combined with two-dimensional liquid and gas distribution models for a packed column in the offshore environment. Pilot experiments were conducted for an NaOH-air absorption system to obtain experimental data for determining the effect of tilt angle on absorption performances. By introducing key parameters, the proposed model can describe the experimental data well. The internal behavior of a tilted packed column in the 2D domain was analyzed in terms of liquid distribution, gas distribution, effective surface area, and CO_2 concentration. Two metrics were introduced to quantify the effect of tilt angle on absorption performance: mass transfer efficiency and absorption efficiency. Under the considered operating conditions, the mass transfer efficiency decreased to approximately 0.85. Absorption efficiency is a function of column dimensions, including column height and diameter. The absorption efficiency can be directly used to estimate a design value for the packed height of a tilted column. A deep packed height induces further detrimental tilt effects on absorption performance due to the worsened liquid and gas mal-distribution. This ability to describe absorption performance considering column dimensions could allow the proposed model to act as a predictive design tool for a tilted packed column if they are to be developed further. Finally, we noted that the proposed model can be applied to any systems other than air-water system (e.g., CO_2-amine solution system for acid gas removal) by updating physical properties, such as surface tension and viscosity.

ACKNOWLEDGEMENT

This work was supported by the National Research Foundation of Korea (NRF) grant funded by the Korea government (MSIT) (2018R1C1B6009074).

NOMENCLATURE

Abbreviations

CFD : computational fluid dynamics
FLNG : floating liquefied natural gas
LGDM : liquid and gas distribution model
LNG : liquefied natural gas
NCCM : networked column compartment model
PP : polypropylene
SS : stainless steel
VSD : vertical sub-column dimension

Parameters and Variables

A_G : matrix of gas flow rates
a : specific (geometric) area of packing [m^2/m^3]
a_e : effective surface area [m^2/m^3]
C_{OH^-} : concentration of hydroxide ion [mol/L]
D_{sub} : diameter of a sub-column [m]
$D_{CO_2,L}$: diffusion coefficient of CO_2 in the liquid phase [m_2/s]
$D_{CO_2,W}$: diffusion coefficient of CO_2 in water [m_2/s]
d_h : hydraulic diameter of packing [m]
G : gas flow rate [m^3/hr]
H_{sub} : packed height of a sub-column [m]
H_{CO_2} : Henry's constant [m^3Pa/kmol]
H_{CO_2-PM} : Henry's constant in Pohorecki and Moniuk [27] [kmol/m^3/bar]
$H_{CO_2,w-PM}$: Henry's constant in water in Pohorecki and Moniuk [27] [kmol/m^3/bar]
h_i : Barrett contributions in Henry's constant i=Na^+, OH^-, CO_3^{2-}, CO_2 [L/mol]
I : ionic strength [mol/L]
i : packed height index [-]
j : tilt-axis index [-]
K_G : overall mass transfer coefficient [kmol/m^2/Pa/s]
K_{exp} : the number of experimental runs [-]
$k_g^{'}$: liquid film mass transfer coefficient [kmol/m^2/Pa/s]
k_1 : pseudo-first order rate constant [1/s]
k_{OH^-} : second-order reaction rate constant [m^3/kmol/s]
$k_{OH^-}^{\infty}$: second-order reaction rate constant at infinite dilution [m^3/kmol/s]
L : liquid flow rate [m^3/hr]
N : column bottom index of packed height index
R : ideal gas constant, 8314.5 [m^3Pa/kmol/K]
T : liquid temperature [°C]
u_G : gas velocity [m/s]
u_L : liquid velocity [m/s]
v_L : kinematic viscosity [cp]
X : decision variable vector
x_G : gas ratio vector
y_k : experimental measurement of CO_2 at the outlet at k^{th} experimental run [-]
y_k^{NCCM} : NCCM result of CO_2 at the outlet at k^{th} experimental run [-]
$y_{CO_2,in}$: CO_2 mole fraction at the inlet [-]
$y_{CO_2,out}$: CO_2 mole fraction at the outlet [-]

Greek Letters

α : gas split ratio [-]
λ_i : adjustable parameters for effective surface area [-]
μ_L : dynamic liquid viscosity [cp]
μ_w : dynamic water viscosity at 20 °C [cp]
θ : permanent tilt angle [°]
η_{mte} : mass transfer efficiency
η_{ae} : absorption efficiency
ρ_L : liquid density [kg/m^3]
σ_L : surface tension of liquid [N/m]

REFERENCES

1. K. Park, W. Won and D. Shin, *J. Nat. Gas. Sci. Eng.*, **34**, 958 (2016).
2. S. Tesch, T. Morosuk and G. Tsatsaronis, *Energy*, **117**, 550 (2016).
3. H. Zhang, Y. Liang, Q. Liao, X. Yan, Y. Shen and Y. Zhao, *Energy*, **133**, 424 (2017).
4. W. Won, S. K. Lee, K. Choi and Y. Kwon, *Korean J. Chem. Eng.*,

31, 732 (2014).
5. W. H. Zhao, J. M. Yang, Z. Q. Hu and Y. F. Wei, *Ocean. Eng.*, **38**, 1555 (2011).
6. Y. Son and W. Won, *Chem. Eng. Sci.*, **195**, 894 (2019).
7. J. Lee, J. Kim, H. Kim, K. S. Lee and W. Won, *J. Nat. Gas. Sci. Eng.*, **61**, 206 (2019).
8. J. Lee, Y. Son, K. S. Lee and W. Won, *Energies*, **12**, 852 (2019).
9. J. F. Billingham and M. J. Lockett, *Chem. Eng. Res. Des.*, **80**, 373 (2002).
10. J. T. Cullinane, N. Yeh and E. Grave, Brasil Offshore Conference and Exhibition, Macaé, Brazil, SPE (2011).
11. L. Klemas and J. A. Bonilla, *Chem. Eng. Prog.*, **91**, 27 (1995).
12. J. W. Mullin, *Chem. Eng. Prog.*, **33**, 408 (1957).
13. M. Schultes, *Ind. Eng. Chem. Res.*, **39**, 1381 (2000).
14. J. Stichlmair and A. Stemmer, *Inst. Chem. Eng. Symp. Ser.*, **104**, 213 (1987).
15. B. Hanley, *Sep. Purif. Technol.*, **16**, 7 (1999).
16. R. E. Manning and M. R. Cannon, *Ind. Eng. Chem.*, **49**, 347 (1957).
17. I. Iliuta and F. Larachi, *AIChE J.*, **63**, 1064 (2017).
18. D. A. Pham, Y.-I. Lim, H. Jee, E. Ahn and Y. Jung, *AIChE J.*, **61**, 4412 (2015).
19. Y. Son, S. Lee, S. Han, D. Yang, K. Min and K. S. Lee, *Chem. Eng. Sci.*, **182**, 1 (2018).
20. R. Billet and M. Schultes, *Chem. Eng. Res. Des.*, **77**, 498 (1999).
21. R. E. Tsai, Ph.D. Thesis. The University of Texas at Austin (2010).
22. S. Bishnoi and G. T. Rochelle, *Chem. Eng. Sci.*, **55**, 5531 (2000).
23. P. V. Danckwerts and A. Lannus, *J. Electrochem. Soc.*, **117**, 369C (1970).
24. J. Haubrock, J. A. Hogendoorn and G. F. Versteeg, *Int. J. Chem. React. Eng.*, **3**, 1 (2005).
25. L. Kucka, E. Y. Kenig and A. Górak, *Ind. Eng. Chem. Res.*, **41**, 5952 (2002).
26. R. E. Tsai, A. F. Seibert, R. B. Eldridge and G. T. Rochelle, *AlChE J.*, **57**, 1173 (2011).
27. R. Pohorecki and W. Moniuk, *Chem. Eng. Sci.*, **43**, 1677 (1988).
28. W. Moniuk and R. Pohorecki, *Hung. J. Ind. Chem.*, **19**, 175 (1991).
29. P. V. L. Barrett, Ph.D. Thesis. University of Cambridge (1969).
30. W. Won and J. Kim, *Comput. Chem. Eng.*, **96**, 87 (2017).
31. W. Won and K. S. Lee, *Chem. Eng. Sci.*, **162**, 21 (2017).
32. Y. Son, G. Kim, S. Lee, H. Kim, K. Min and K. S. Lee, *Chem. Eng. Sci.*, **166**, 168 (2017).
33. D. Perry, D. E. Nutter and A. Hale, *Chem. Eng. Prog.*, **86**, 30 (1990).